Titanium(IV) Inclusion as a Versatile Route to Photoactivity in Metal–Organic Frameworks

Jenna L. Mancuso and Christopher H. Hendon*

Titanium-containing metal–organic frameworks (MOFs) are known to perform light-promoted chemical transformations. Formation of these frameworks, accessed either natively or via transmetallation, can instill beneficial photocatalytic properties in previously photo-inert scaffolds. Band edge diagrams coupled with their density of states illustrate the persistent nature of the accessible titanium d-states at the conduction band edge, independent of linker identity. In essentially all of these Ti-containing frameworks, the valence band edge localizes on the organic component, permitting facile modulation of the band gap. In sum, the spatial separation of photogenerated excitons will be observed in both the native and titanium(IV)-substituted MOFs, and this exciton pair is useful in photocatalysis.

Photocatalysts offer a unique advantage over conventional thermal catalysts as they harness a ubiquitous source of energy, light, to perform chemical transformations. Photocatalytic materials absorb photons equal to, or greater than, their band gap energy to produce high-energy electrons and low-energy holes.[1] These charges may then perform oxidative and reductive chemistry enabling applications in water purification,[2,3] renewable fuel generation,[4–6] and CO_2 conversion.[7–9] The prospect of solar-to-chemical energy conversion for both catalytic and energy applications makes development of new scaffolds that absorb visible light to promote novel single and multielectron redox processes a key synthetic target.[10]

In general, the desired attributes for a photocatalyst are i) a narrow band gap enabling the absorption of photons in the visible range; ii) valence and conduction band edges aligned with reactant potentials for efficient electron transfer upon excitation; iii) long exciton lifetimes to reduce competition between recombination and the desired catalytic transformation; and iv) an ability to modulate reactivity and selectivity by altering the structure and composition. Transition metal oxides possess some of these desirable attributes.[11] Their elemental diversity and various accessible oxidation states provide a medley of transition metal oxides to select for a given catalytic function.[7,12]

J. L. Mancuso, Prof. C. H. Hendon
Materials Science Institute
Department of Chemistry and Biochemistry
University of Oregon
Eugene, OR 97403, USA
E-mail: chendon@uoregon.edu

The ORCID identification number(s) for the author(s) of this article can be found under https://doi.org/10.1002/adts.201900126

TiO_2 is the champion photocatalyst because of its high efficiency and stability, low cost and toxicity, and earth abundance.[13] When irradiated, Ti[III] is formed through charge transfer from oxygen to titanium.[14,15] This separation of electron–hole pairs enables redox processes such as photodegradation of organic dyes[15,16] and renewable fuel production.[4] The large electronic band gap (3.0 eV),[17] however, limits the usable wavelengths from the solar spectrum. Efforts to close the electronic band gap through compositional and morphological alterations have been successful.[18,19] However, manipulation of rigid inorganic lattices can be synthetically difficult and leads to adverse effects such as material instabilities or high recombination rates near defects.[20] TiO_2 could thus be improved upon by designing a material with similar, but more readily tunable, electronic properties.

MOFs are a class of compositionally diverse, high surface area, crystalline materials. Some embodiments contain metal-oxide clusters (i.e., nodes) crystallographically orders and separated by anionic organic linkers. MIL-125,[21] for example, is constructed from $[Ti_8O_8(OH)_4]^{12+}$ inorganic building blocks interconnected by benzene dicarboxylate (BDC) linkers. Like TiO_2, the conduction band edge is dominated by titanium d-states; photoexcitation yields a transient Ti[III] (**Figure 1**).[22] Unlike TiO_2, the valence band edge of MIL-125 is localized on an organic source of titanium-bound oxygen, BDC. Further, inherent MOF porosity facilitates valuable trapping of the low-valent titanium species through bulk reduction of the framework by small molecules in the pore. Addition of up to eight electrons per node can be achieved in the presence of charge stabilizing counterions.[23,24]

While both TiO_2 and MIL-125 have native band gaps in the UV, the valence band of MIL-125 can be tailored through organic substitution. Amino functionalization of the BDC linker brings the optical gap into the visible range (a reduction in band gap by approximately 1.5 eV), intensifying the harvestable solar wavelengths—a phenomenon reminiscent of nitrogen-doping in anatase TiO_2.[25–27] Varying the electron donating ability of organic functional groups enables higher fidelity band gap tunability.[28] Independent of the functional group, the conduction band edge remains unaltered, and the lowest energy exciton is spatially separated. In other words, the optical gap is attributed to a linker-to-metal charge transfer (LMCT). Separated Ti[III] species and valence band holes are then poised to perform reduction (e.g., Cr(VI)-to-Cr(III)[29]) or oxidation (e.g., amines-to-imines[30]), respectively. The reactivity of MIL-125
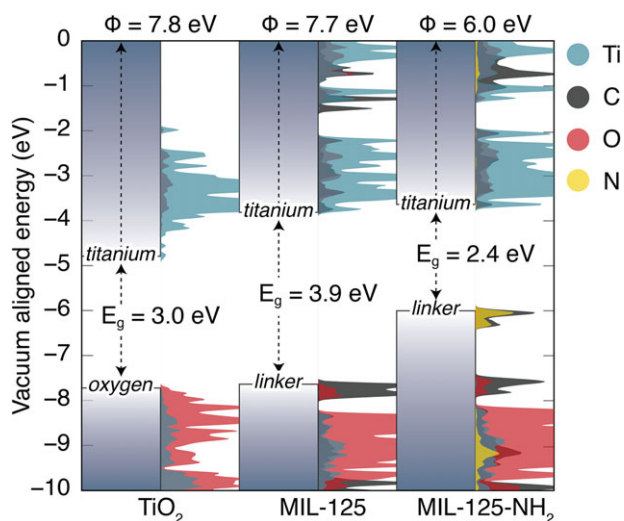
ADVANCED
SCIENCE NEWS
www.advancedsciencenews.com

ADVANCED
THEORY AND
SIMULATIONS
www.advtheorysimul.com

Figure 1. Band edge diagrams and theoretical density of states for TiO_2, MIL-125, and MIL-125-NH_2 show the familiar MOF confinement effects (wider band gap with reduced dimensionality of the metal-oxide cluster compared to bulk). Amino-functionalization is presented to demonstrate that because MOFs feature organic valence bands, additional BDC functionality affects their energetics.

thus parallels TiO_2, but has the advantages of inherent porosity (enabling higher active site accessibility) and electronic customizability (allowing band gap tunability and energy level matching).

Other Ti^{IV}-containing MOFs (e.g., NTU-9,[31] COK-69,[32] PCN-415[33]) demonstrate photoactivity similar to MIL-125—it is the metal ion, Ti^{IV}, that makes these frameworks unique. MOFs composed of BDC and other d^0 group 4 metals (i.e., Zr^{IV} or Hf^{IV}) do not feature the same reactivity because the unoccupied Zr and Hf orbitals lay closer to the vacuum level—their conduction bands are localized on their organic motifs.[34–36] Thus, there remains value in the development of new scaffolds consisting of Ti^{IV}. This may be achieved in two ways; i) construct new scaffolds featuring Ti^{IV} through direct syntheses,[33] or ii) coalesce the favorable properties of an existing framework, such as pore size or water stability, with Ti^{IV} character through transmetallation. In both cases, the question remains whether Ti^{IV} will define the conduction band independent of MOF structure or composition.

Despite the relative maturity of metal-exchange procedures, there are surprisingly few examples of Ti^{IV}-substituted MOFs.[37] Ti^{III}, however, undergoes more facile exchange (e.g., Zn^{II}-MOF-5[38] has been successfully transmetallated with Ti^{III}, but there are no reports of Ti^{IV}-MOF-5 to date)[39] and, once incorporated, can be oxidized by a single electron to the desired form.[40] It should be noted that titanium can be incorporated into seemingly non-exchangeable MOFs (e.g., UiO-66 and other ceramics) by appendage through atomic layer deposition and wet impregnation, but the inner-shell Ti^{IV} ligands then depend on the synthetic conditions.[34,41] In principle these Ti^{IV} could also be photoactive, but position of the unoccupied titanium orbitals demonstrate a mild dependence on the non-MOF ligands. In any case, transmetallation or direct synthetic approaches to incorporating Ti^{IV} may be a worthwhile endeavor for the development of novel photocatalysts.

Developing design principles such as targeting scaffolds with organic valence and Ti-conduction band character can narrow the vast chemical space of potential photoactive MOFs. Density functional theory is useful for this, as photocatalytic function is derived from the material band gap and exciton localities—both are properties readily obtained from theory.[42] Thus, this study seeks to demonstrate that metal-exchanged systems containing Ti^{IV} are interesting synthetic targets because organic valence bands and Ti-centered conduction bands subsist indepedent of MOF structure of composition.

To begin, the effect of ligand identity and MOF structure on the energetics of Ti^{IV} must be decoupled. A series of BDC-containing MOFs MOF-5, MIL-125, PCN-415, Zr^{IV}- and Hf^{IV}-UiO-66[35,36] were selected as candidates to compare the native $Ti^{(IV)}$ containing scaffolds (i.e. MIL-125, PCN-415) with transmetallated variants (e.g. Ti-MOF-5).[40,43] Other non-BDC based frameworks, MOF-74 and MFU-4l, were then selected as scaffolds to isolate the importance of ligand environment on the transmetallated Ti orbitals. These transmetallated frameworks are presented in contrast to other native Ti-containing scaffolds; COK-69, NTU-9.

From the HSEsol06 level of theory[44] (using the procedure detailed in the Experimental Section), band edge diagrams and corresponding DOS plots were obtained for each of the native Ti^{IV}-MOFs (**Figure 2**). Analogous to TiO_2, the DOS of each native titanium-containing MOF features a conduction band minimum (CBM) centered on titanium. The workfunction and parentage of the valence band maximum (VBM) for all species are additionally localized on the linker. The BDC valence of PCN-415 lays somewhere between that of MIL-125 and Zr^{IV}/Hf^{IV}-UiO-66, attributed to the fact that PCN-415 has a hybrid node consisting of both Ti^{IV} and Zr^{IV}. Thus, the valence band energy is somewhat determined by the relative Lewis acidity of the node. In comparison, the conduction bands of both Zr^{IV} and Hf^{IV} BDC derivatives lack photoaccessible metal-based states despite their d^0 configuration (Figure 2), indicating that a ligand-to-ligand transition is favored for hafnium- and zirconium-bound MOFs. This produces neither spatial separation nor stable excited organic radicals, and consequently low photocatalytic activity.

The real utility of Ti^{IV} would be realized if the conduction band of any transmetallated MOF was persistently centered on Ti, independent of the ligand scaffold surrounding it. Fortunately, there is a wealth of experimental and theoretical literature that demonstrate the emergence of conduction band states centered on titanium in these scenarios. The resultant LMCT is predicted by DOS plots[45–47] and electronic band diagrams[48,49] from DFT performed by other groups and evidenced experimentally by a range of spectroscopic methods.[40,50–54] Thus, transmetallation of MOFs with an organic VBM presents an opportunity to instill the beneficial photocatalytic property of long-lived, spatially separated excitons, formed with a tunable wavelength, in virtually any scaffold. However, remembering the distinct lack of literature on Ti^{IV}-transmetallated frameworks, a careful selection of transmetallated frameworks can be used to paint a comprehensive picture of the persistence of Ti-orbitals in otherwise Ti-free materials by computing the electron energetics of MOFs whose ligands impose vastly different field strengths.

MOF-5, Zn-MOF-74, and MFU-4l feature native ligand-to-ligand transitions because Zn^{II} is d^{10}, placing the next unoccupied metal-centered orbital far above the CBM (+1.6 eV greater
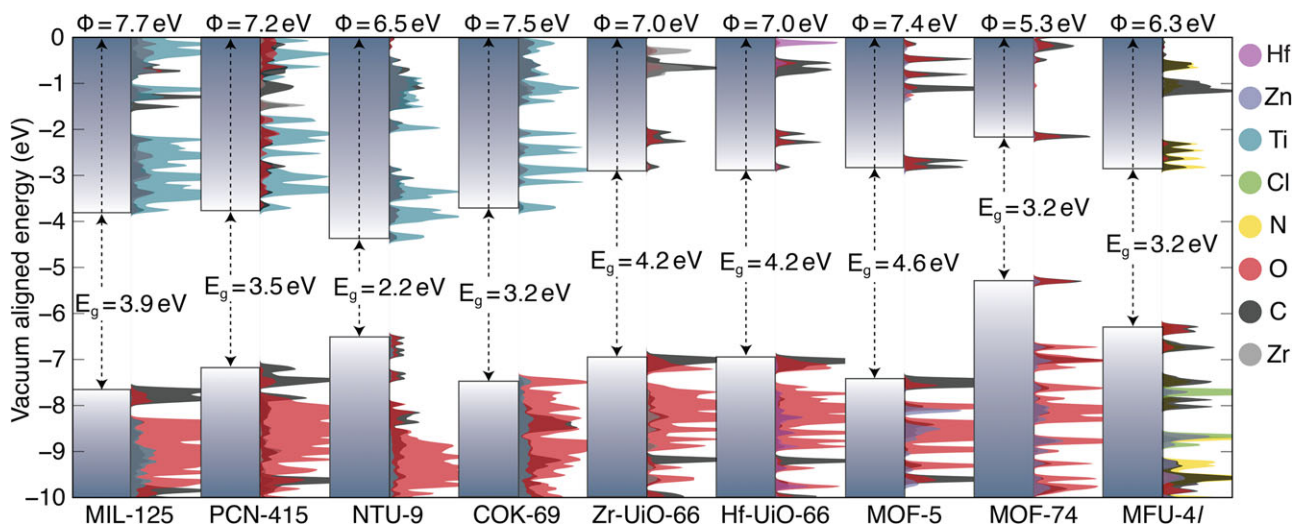
ADVANCED
SCIENCE NEWS
www.advancedsciencenews.com

ADVANCED
THEORY AND
SIMULATIONS
www.advtheorysimul.com

Figure 2. Ti orbitals define the conduction band in Ti-based MOFs. Other non-Ti MOFs (e.g., Zr^{IV} and Hf^{IV}-UiO-66, MOF-5, MOF-74, and MFU-4*l*) feature higher energy, organic-centered conduction bands that are less ideal for photocatalysis. In all cases, the valence bands are composed of linker-centered orbitals.

than the electron affinity of bulk MOF-5, +1.5 eV for bulk Zn-MOF-74, and +1.8 eV for bulk MFU-4*l*). However, each framework is known to maintain structural integrity through post-synthetic metal exchange,[40,55,56] and BDC and triazole lay on either end of the ligand field spectrum. The propensity for Ti^{IV} to form octahedral coordination environments mandated that Ti^{IV}-substituted MOF-74, MFU-4*l*, and MOF-5 require additional ions and neutral ligands. Our selection is presented in **Figure 3**; in sum, Cl^- and H_2O were added to achieve charge neutrality and octahedral coordination.

The persistence of Ti^{IV} states defining the CBM in transmetallated frameworks without perturbing the valence band (Figure 3) is particularly remarkable as the Ti-orbitals again lay midgap relative to the organic orbitals, independent of ligand field strength. More importantly, despite the differences in ligand field strength, the Ti-orbitals in MIL-125, PCN-415, COK-69, Ti^{IV}-MOF-5, Ti^{IV}-MOF-74, NTU-9, and Ti^{IV}-MFU-4*l* all have similar electron affinities (≈ 4 eV), fluctuating due to variation in ligand field strength,[57] suggesting that one could target similar photocatalytic transformations by simply installing Ti^{IV} in essentially any metal-cluster based MOF without dramatically changing its reductive ability.

The incorporation of titanium can thus be viewed as a comprehensive design route to metal-based frontier conduction bands; the modular nature of valence band energetics should not be overlooked. It is their reducing power that determines the ability to "photodope" the framework (i.e., store electrons in the conduction band via excitation and subsequent reduction of the framework-bound hole with an extrinsic reductant). Considering the general scheme of MOF photoactivity shown in **Figure 4**, excitation followed by framework reduction results in the storage of electrons in the conduction band only if the rate of reduction is faster than that of exciton recombination. These rates are determined partially by spatial separation of the electron and hole (a property related to the structure of the MOF itself), and the energetics of the hole in the valence band (a property related to the
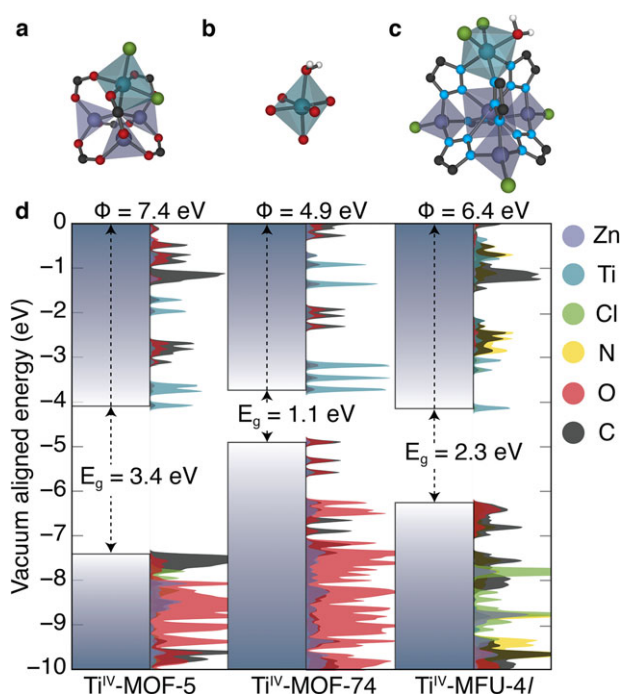

Figure 3. Ti^{IV}-substituted nodes of the post-synthetically exchangeable MOFs. a) MOF-5, b) MOF-74, and c) MFU-4*l* are passivated with adventitious Cl^- and H_2O. d) Their electron energy diagrams and density of states reveal that titanium-based states define the conduction band extrema in all frameworks, supporting the hypothesis that its incorporation will generally provide access to LMCT from organic-based VBMs.

identity of the ligand). Recombination rates are usually unfavorably fast in frameworks where the valence and conduction band edges are centered on organics.[22] Thus, while the linker appears to play a relatively benign role in determining the conduction band energetics of Ti-based MOFs, the valence band does play
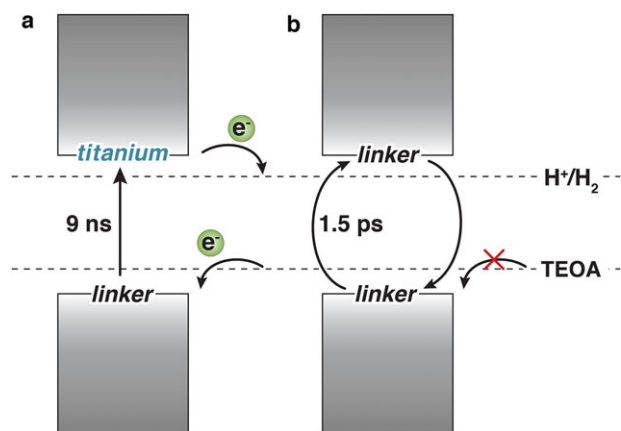
ADVANCED
SCIENCE NEWS

www.advancedsciencenews.com

ADVANCED
THEORY AND
SIMULATIONS

www.advtheorysimul.com

Figure 4. a) MOF systems with long-lived excitons (i.e., LMCT), such as MIL-125, facilitate photodoping and catalytic reduction via Ti^{IV}. b) Scaffolds with highly localized excitations, such as UiO-66, recombine faster than catalytic redox can occur.

an operative role in the photocatalytic activity of a given MOF, particularly when looking beyond single electron photocatalytic processes.

In sum, the results presented here demonstrate that metal-exchanged MOFs exhibit similar properties to those that are natively constructed from titanium. Independent of ligand field (where carboxylates and triazoles represent extremes in ligand field strength), titanium orbitals sit mid-gap, relative to the organic orbitals. As a result, metal-exchange becomes a very important strategy to accessing photocatalytic frameworks otherwise unattainable through direct approaches. Furthermore, the utility of Ti^{IV} in MOF-based photocatalysts lays the foundation for other studies of equally rare high-valent metal compositions (e.g., Fe^{III}, V^V, etc.) Other metal-oxide clusters, including zirconium and hafnium-based nodes, feature linker-centered frontier states when interconnected by organic components. Titanium can hence be viewed as a unique element to target MOF photoactivity due to its predictable energetic positioning. Experimentalists are encouraged to continue in pursuit of Ti^{IV}-containing frameworks (either through direct routes or transmetallation) as it is both the ligand and metal that contribute to the framework's ability to perform photocatalysis/multielectron energy storage. Continuing investigation of these modular scaffolds will reveal fundamental principles for general photocatalyst design.

Experimental Section

All structures were optimized with PBEsol[58] as implemented in VASP[59–61] using the PAW plane wave method[62] and a 500 eV plane-wave cutoff basis set. A Γ centered $2 \times 2 \times 2$ k-grid was converged to ionic and electronic criteria of 0.005 eV and 1×10^{-6} eV, respectively. The HSEsol06[44] (PBEsol+25% HF) level of theory was used to recover more accurate band-gap energies using the same convergence criteria, and a Γ-only sampling of the first Brillouin zone. Parent scaffolds were fully optimized and aligned to vacuum using a previously reported method.[63] For metal-substituted derivatives, one metal per unit cell was exchanged, and the unit cell shape and volume were constrained to the parent framework parameters over the course of the optimization. Titanium was kept in the 4+ oxidation state by including chlorides in its coordination sphere, sat-

urating the octahedral environment with water in the case of MFU-4l. For MOF-74, two electrons were removed from the unit cell and the vacant coordination site was again passivated with water. Metal substitution resulted in a dipole across the unit cell, preventing accurate vacuum level alignment. Thus, the lowest native metal orbital in the conduction band of each substituted material was aligned to that of the parent material. This strategy is based on the assumption that native metal orbitals of the remote unsubstituted node will be negligibly perturbed by metal-exchange due to the insulating nature of metal–oxygen bonds.

Conflict of Interest

The authors declare no conflict of interest.

[1] T. P. Yoon, M. A. Ischay, J. Du, *Nat. Chem.* **2010**, *2*, 527.
[2] C. Lettmann, H. Hinrichs, W. F. Maier, *Angew. Chem., Int. Ed.* **2001**, *40*, 3160.
[3] A. Mills, R. H. Davies, D. Worsley, *Chem. Soc. Rev.* **1993**, *22*, 417.
[4] A. Fujishima, K. Honda, *Nature*, **1972**, *238*, 37.
[5] C. Ampelli, G. Centi, R. Passalacqua, S. Perathoner, *Energy Environ. Sci.* **2010**, *3*, 292.
[6] K. S. Joya, Y. F. Joya, K. Ocakoglu, R. van de Krol, *Angew. Chem., Int. Ed.* **2013**, *52*, 10426.
[7] S. Navalón, A. Dhakshinamoorthy, M. Álvaro, H. Garcia. *ChemSusChem* **2013**, *6*, 562.
[8] D. Kim. K. K. Sakimoto, D. Hong, P. Yang, *Angew. Chem., Int. Ed. 54*, **2015**, 3259.
[9] M. Tahir, N. S. Amin, *Renewable Sustainable Energy Rev.* **2013**, *25*, 560.
[10] L. Marzo, S. K. Pagire, O. Reiser, B. König, *Angew. Chem., Int. Ed.* **2018**, *57*, 10034.
[11] M. M. Khan, S. F. Adil, A. Al-Mayouf, *J. Saudi Chem. Soc.* **2015**, *19*, 462.
[12] M. C. Toroker, D. K. Kanan, N. Alidoust, L. Y. Isseroff, P. Liao, E. A. Carter, *Phys. Chem. Chem. Phys.* **2011**, *13*, 16644.
[13] N. S. Allen, M. Edge, J. Verran, L. Caballero, C. Abrusci, J. Stratton, J. Maltby, C. Bygott *Open Mater. Sci. J.* **2010**, *3*, 6.
[14] H. Ariga, T. Taniike, H. Morikawa, M. Tada, B. K. Min, K. Watanabe, Y. Matsumoto, S. Ikeda, K. Saiki, Y. Iwasawa, *J. Am. Chem. Soc.* **2009**, *131*, 14670.
[15] R. F. Howe, M. Gratzel, *J. Phys. Chem.* **1987**, *91*, 3906.
[16] M. Xing, W. Fang, M. Nasir, Y. Ma, J. Zhang, M. Anpo, *J. Catal.* **2013**, *297*, 236.
[17] D. O. Scanlon, C. W. Dunnill, J. Buckeridge, S. A. Shelvin, A. J. Logsdail, S. M. Woodley, C. R. A. Catlow, M. J. Powell, R. G. Palgrave, I. P.

Parkin, G. W. Watson, T. W. Keal, P. Sherwood, A. Walsh, A. A. Sokol, *Nat. Mater.* **2013**, *12*, 798.

[18] M. Anpo, M. Takeuchi, *J. Catal.* **2003**, *216*, 505.

[19] J. F. Guayaquil-Sosa, B. Serrano-Rosales, P. J. Valadés-Pelayo, H. de Lasa, *Appl. Catal., B* **2017**, *211*, 337.

[20] M. D. Hernández-Alonso, F. Fresno, S. Suárez, J. M. Coronado, *Energy Environ. Sci.* **2009**, *2*, 1231.

[21] M. Dan-Hardi, C. Serre, T. Frot, L. Rozes, G. Maurin, C. Sanchez, G. A. Férey, *J. Am. Chem. Soc.* **2009**, *131*, 10857.

[22] M. A. Nasalevich, C. H. Hendon, J. G. Santaclara, K. Svane, B. van der Linden, S. L. Veber, M. V. Fedin, A. J. Houtepen, M. A. van der Veen, F. Kapteijn, A. Walsh, J. Gascon, *Sci. Rep.* **2016**, *6*, 23676.

[23] C. T. Saouma, S. Richards, S. Smolders, M. F. Delley, R. Ameloot, F. Vermoortele, D. E. De Vos, J. M. Mayer, *J. Am. Chem. Soc.* **2018**, *140*, 16184.

[24] C. T. Saouma, C. C. Tsou, S. Richard, R. Ameloot, F. Vermoortele, S. Smolders, B. Bueken, A. G. DiPasquale, W. Kaminsky, C. N. Valdez, D. E. De Vos. J. M. Mayer, *Chem. Sci.* **2019**, *10*, 1322.

[25] Y. Fu, D. Sun, Y. Chen, R. Huang, Z. Ding, X. Fu, Z. Li, *Angew. Chem., Int. Ed.* **2012**, *51*, 3364.

[26] M. B. Chambers, X. Wang, L. Ellezam, O. Ersen, M. Fontecave, C. Sanchez, L. Rozes, C. Mellot-Draznieks, *J. Am. Chem. Soc.* **2017**, *139*, 8222.

[27] C. Di Valentin, G. Pacchioni, A. Selloni, *Phys. Rev. B* **2004**, *70*, 085116.

[28] C. H. Hendon, D. Tiana, M. Fontecave, C. Sanchez, L. D'arras, C. Sassoye, L. Rozes, C. Mellot-Draznieks, A. Walsh, *J. Am. Chem. Soc.* **2013**, *135*, 10942.

[29] H. Wang, X. Yuan, Y. Wu, G. Zeng, X. Chen, L. Leng, Z. Wu, L. Jian, H. Li, *J. Hazard. Mater.* **2015**, *286*, 187.

[30] D. Sun, L. Ye, Z. Li, *Appl. Catal., B* **2015**, *164*, 428.

[31] J. Gao, J. Miao, P. Z. Li, W. Y. Teng, L. Yang, Y. Zhao, B. Liue, Q. A. Zhang, *Chem. Commun.* **2014**, *50*, 3786.

[32] B. Bueken, F. Vermoortele, D. E. P. Vanpoucke, H. Reinsch, C.-C. Tsou, P. Valvekens, T. De Baerdemaeker, R. Ameloot, C. E. A. Kirschhock, V. Van Speybroeck, J. M. Mayer, D. De Vos. *Angew. Chem., Int. Ed.* **2015**, *54*, 13912.

[33] S. Yuan, J.-S. Qin, H.-Q. Xu, J. Su, D. Rossi, Y. Chen, L. Zhang, C. Lollar, Q. Wang, H.-L. Jian D.-H. Son, H. Xu, Z. Huang, X. Zou, H.-C. Zhou. *ACS Cent. Sci.* **2018**, *4*, 105.

[34] J. G. Santaclara, A. I. Olivos-Suarez, A. Gonzalez-Nelson, D. Osadchii, M. A. Nasalevich, M. A. van der Veen, F. Kapteijn, A. M. Sheveleva, S. L. Veber, M. V. Fedin, A. T. Murray, C. H. Hendon, A. Walsh, J. Gascon, *Chem. Mater.* **2017**, *29*, 8963.

[35] J. H. Cavka, S. Jakobsen, U. Olsbye, N. Guillou, C. Lamberti, S. Bordiga, K. P. Lillerud, *J. Am. Chem. Soc.* **2008**, *130*, 13850.

[36] S. Jakobsen, D. Gianolio, D. S. Wragg, M. H. Nilsen, H. Emerich, S. Bordiga, C. Lamberti, U. Olsbye, M. Tilset, K. P. Lillerud, *Phys. Rev. B* **2012**, *86*, 125429.

[37] M. Kim, J. F. Cahill, H. Fei, K. A. Prather, S. M. Cohen, *J. Am. Chem. Soc.* **2012**, *134*, 18082.

[38] N. L. Rosi *Science*, **2003**, *300*, 1127.

[39] C. K. Brozek, M. Dincă, *J. Am. Chem. Soc.* **2013**, *135*, 12886.

[40] L. Zou, D. Feng, T.-F. Liu, Y.-P. Chen, S. Yuan, K. Wang, X. Wang, S. Fordham, H.-C. Zhou, *Chem. Sci.* **2016**, *7*, 1063.

[41] J. E. Mondloch, W. Bury, D. Fairen-Jimenez, S. Kwon, E. J. DeMarco, M. Weston, A. A. Sarjeant, S. T. Nguyen, P. C. Stair, R. Q. Snurr, O. K. Farha, J. T. Hupp, *J. Am. Chem. Soc.* **2013**, *135*, 10294.

[42] M. A. Syzgantseva, C. P. Ireland, F. M. Ebrahim, B. Smit, O. A. Syzgantseva, *J. Am. Chem. Soc.* **2019**, *141*, 6271.

[43] R. J. Comito, K. J. Fritzsching, B. J. Sundell, K. Schmidt-Rohr, M. Dincă, *J. Am. Chem. Soc.* **2016**, *138*, 10232.

[44] A. V. Krukau, O. A. Vydrov, A. F. Izmaylov, G. E. Scuseria, *J. Chem. Phys.* **2006**, *125*, 224106.

[45] A. Walsh, C. R. A. Catlow, *ChemPhysChem* **2010**, *11*, 2341.

[46] S. Wang, T. Kitao, N. Guillou, M. Wahiduzzaman, C. Corcos-Martineau, F. Nouar, A. Tissot, L. Binet, N. Ramsahye, S. Devautour-Vinot, S. Kitagaw, S. Seki, Y. Tsutsui, V. Briois, N. Steunou, G. Maurin, T. Uemura, C. Serre, *Nat. Commun.* **2018**, *9*, 1660.

[47] N. M. Padial, J. Castells-Gil, N. Almora-Barrios, M. Romero-Angel, I. da Silva, M. Barawi, A. García-Sánchez, V. A. de la Peña O'Shea, C. Martí-Gastaldo, *J. Am. Chem. Soc.* **2019**, https://doi.org/10.1021/jacs.9b04915.

[48] T. Komatsu, J. M. Taylor, H. Kitagawa, *Inorg. Chem.* **2016**, *55*, 546.

[49] D. Sun, W. Liu, M. Qiu, Y. Zhang, Z. Li, *Chem. Commun.* **2015**, *51*, 2056.

[50] Y. Keum, S. Park, Y.-P. Chen, J. Park, *Angew. Chem., Int. Ed.* **2018**, *57*, 14852.

[51] H. Assi, L. C. Pardo-Pérez, G. Mouchaham, F. Ragon, M. Nasalevich, N. Guillou, C. Martineau, H. Chevreau, F. Kapteijn, J. Gascon, P. Fertey, E. Elkaim, C. Serre, T. Devic, *Inorg. Chem.* **2016**, *55*, 7192.

[52] S. Yuan, T.-F. Liu, D. Feng, J. Tian, K. Wang, J. Qin, Q. Zhang, Y.-P. Chen, M. Bosch, L. Zou, S. J. Teat, S. J. Dalgarno, H.-C. Zhou, *Chem. Sci.* **2015**, *6*, 3926.

[53] H. L. Nguyen, F. Gándara, H. Furukawa, T. L. H. Doan, K. E. Cordova, O. M. Yaghi. *J. Am. Chem. Soc.* **2016**, *138*, 4330.

[54] Y. Song, Z. Li, Y. Zhu, X. Feng, J. S. Chen, M. Kaufmann, C. Wang, W. Lin, *J. Am. Chem. Soc.* **2019**, *141*, 12219.

[55] C. K. Brozek, M. Dincă, *Chem. Commun.* **2015**, *51*, 11780.

[56] D. Denysenko, J. Jelic, K. Reuter, D. Volkmer, *Chem. - Eur. J.* **2015**, *21*, 8188.

[57] L. E. Brus, *J. Chem. Phys.* **1984**, *80*, 4403.

[58] J. P. Perdew, K. Burke, M. Ernzerhof, *Phys. Rev. Lett.* **1996**, *77*, 3865.

[59] G. Kresse, J. Furthmüller, *Comput. Mater. Sci.* **1996**, *6*, 15.

[60] G. Kresse, J. Furthmüller, *Phys. Rev. B* **1996**, *54*, 11169.

[61] G. Kresse, J. Hafner, *Phys. Rev. B* **1993**, *47*, 558.

[62] P. E. Blöchl, *Phys. Rev. B* **1994**, *50*, 17953.

[63] K. T. Butler, C. H. Hendon, A. Walsh. *J. Am. Chem. Soc.* **2014**, *136*, 2703.